Liquid Crystals
Publication details, including instructions for authors and subscription information:
http://www.informaworld.com/smpp/title~content=t713926090

Statics and dynamics of wetting: Its contribution to the anchoring of nematics

B. Jérôme[a]; P. Pieranski[a]
[a] Laboratoire de Physique des Solides, Btiment 510, Université de Paris-Sud, Orsay Cedex, France

To cite this Article Jérôme, B. and Pieranski, P.(1989) 'Statics and dynamics of wetting: Its contribution to the anchoring of nematics', Liquid Crystals, 5: 2, 683 — 691
To link to this Article: DOI: 10.1080/02678298908045418
URL: http://dx.doi.org/10.1080/02678298908045418

LIQUID CRYSTALS, 1989, VOL. 5, NO. 2, 683–691

Statics and dynamics of wetting: its contribution to the anchoring of nematics

by B. JÉRÔME and P. PIERANSKI
Laboratoire de Physique des Solides, Bâtiment 510, Université de Paris-Sud, 91405 Orsay Cedex, France

The anchoring of nematics on solid substrates depends both on the nature of the substrate and on the wetting conditions. The second point can be shown by wetting a substrate with nematic droplets. We present the results of wetting experiments on SiO films evaporated under oblique incidence and polymer films rubbed in two orthogonal directions. These two kinds of substrates which have respectively C_S and C_{4v} symmetry, induce bistable anchorings. These results are compared with the predictions of a model of anchoring selection developed previously

1. Introduction: wetting and multistable anchorings of nematics

The wetting of a solid substrate by a liquid is a dynamical process uniting two interfaces (see figure 1): the liquid–air interface acting as a wetting interface, and the solid–air interface which is the surface to wet. These two interfaces unite at the contact line **C**. The motion of this contact line leaves behind the wetted surface (the liquid–solid interface) [1]. This motion results from the flow of the liquid: in the flow pattern the liquid molecules which are at the liquid–air interface move towards the contact line until they reach the solid surface where they come to rest with respect to the substrate [2, 3].

When the liquid is a nematic liquid crystal, the orientation of the molecules at the nematic–air and nematic–solid interfaces are fixed by the anchoring conditions at these interfaces. In general, this results in a different orientation of the nematic on these two interfaces. When the nematic molecules which are at the nematic–air interface move towards the contact line, they interact progressively with the solid substrate. This interaction makes their orientation evolve and finally adopt a direction corresponding to a minimum of the potential of interaction when the molecules reach the solid surface.

When several of these directions exist, i.e. in the case of a multistable anchoring, a choice between the different possible orientations has to be made; it occurs during the evolution of the molecular orientation from that at the nematic–air interface to that at the nematic–solid interface. We have shown [4] that this choice depends on the wetting conditions characterized by the velocity $\mathbf{u}(u, \psi)$ of the contact line **C** or the unit vector $\mathbf{l}(\psi, \delta)$ normal to the wetting surface (see figure 1). The modulus u of the velocity of the contact line and the contact angle are related, so the parameters **u** and **l** are equivalent.

In a previous paper [4] we presented the first results of wetting experiments on SiO films evaporated under oblique incidence. These films induce a bistable anchoring, the asymmetric tilted anchoring for a given range of film thickness and incidence angle of evaporation [5–7]. We have also developed a model of anchoring selection which

0267-8292/89 $3.00

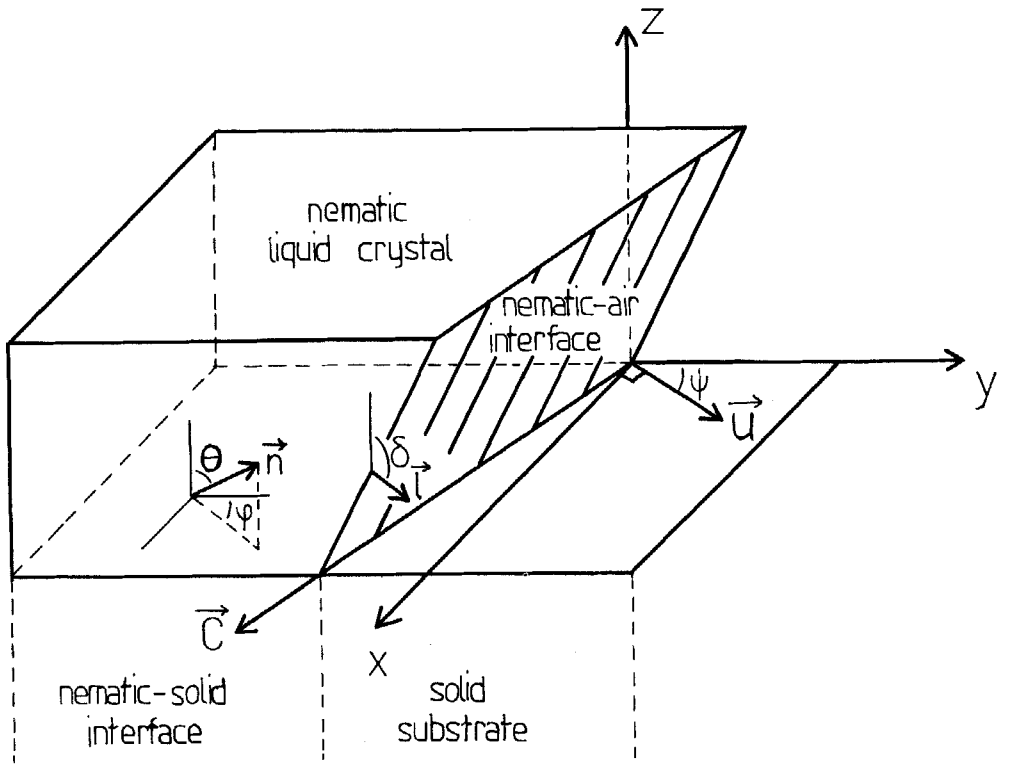

Figure 1. Geometry of wetting.

accounts for the main experimental results. In this paper we present an improved experimental method of wetting, giving results which are more reproducible and more easily comparable with those of our model (§3). We also study the case of an other substrate which induces bistable anchoring: polymer films rubbed in two orthogonal directions (§2).

2. Substrates incuding multistable anchoring

The number and the nature of the different types of anchoring theoretically possible on a given substrate depend on its symmetry, characterized by a space group $G_s = \{g\}$. Each type of anchoring is defined by the set $\{\mathbf{n}_\alpha\}$ of possible anchoring orientations obtained from one orientation $\mathbf{n}_1$ by applying all the symmetry elements of the group G_s: $\mathbf{n}_\alpha = g\mathbf{n}_1$. Different types are obtained according to the position of $\mathbf{n}_1$ with respect to the symmetry elements of the substrate. With this method, we can determine all of the types of anchoring theoretically possible on the two substrates dealt with in this paper.

2.1. *SiO films evaporated under oblique incidence*

These films have a symmetry $C_s = \{E, \hat{\sigma}\}$ where E is the identity and $\hat{\sigma}$ the symmetry in the incidence plane of evaporation σ (see figure 2 (*a*)) [4]. This symmetry allows three types of anchoring according to the orientation of $\mathbf{n}_1$ with respect to σ.

(*a*) In the general case, $\hat{\sigma}\mathbf{n}_1 = \mathbf{n}_2$ is a vector different from $\mathbf{n}_1$ and $-\mathbf{n}_1$. There are two possible anchoring orientations $\{\mathbf{n}_1, \mathbf{n}_2\}$; the anchoring is bistable and is called the asymmetric tilted anchoring.

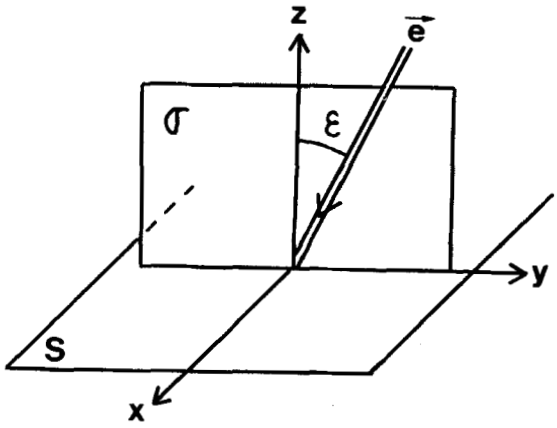

(*a*)

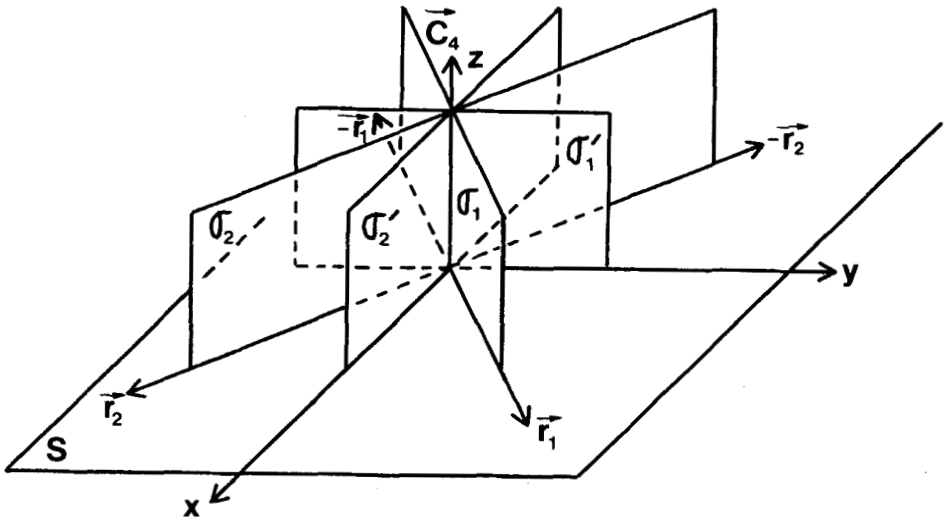

(*b*)

Figure 2. Symmetry elements of substrates. (*a*) SiO films evaporated under oblique incidence. σ = incidence plane; **e** = direction of evaporation. (*b*) Polymer film rubbed in two orthogonal directions. $\mathbf{r}_1$ and $\mathbf{r}_2$ = rubbing directions; σ_1, σ_2, σ_1' and σ_2' = mirror planes; $\mathbf{C}_4$ = fourfold axis.

(*b*) if $\mathbf{n}_1$ belongs to the plane σ, $\hat{\sigma}\mathbf{n}_1 = \mathbf{n}_1$; the anchoring is monostable and is called the symmetric tilted anchoring.

(c) If $\mathbf{n}_1$ is perpendicular to σ, $\hat{\sigma}\mathbf{n}_1 = -\mathbf{n}_1$ which is identical to $\mathbf{n}_1$; the anchoring is monostable and is called the antisymmetric planar anchoring.

We know from previous studies that these three types of anchoring can be observed on SiO films, depending on the thickness of the film [6] and the angle of incidence of the evaporation [5, 7].

2.2. *Polymer films rubbed in two orthogonal directions*

2.2.1. *Experimental achievement of rubbed polymer films*

A film of a solution of polyvinyl alcohol in water (1 per cent by weight) was deposited on a clean glass slide by withdrawing the slide at constant speed, V, from the polymer solution. For a given solution the thickness, d, of the film depends on V [8],

$$d = 0{\cdot}944 \left(\frac{\eta V}{\sigma}\right)^{1/6} \left(\frac{\eta V}{\varrho g}\right)^{1/2},$$

where η is the viscosity of the solution ($\eta = 10^{-3}\,\mathrm{Pa\,s}$), ϱ the specific mass ($\varrho = 10^{-3}\,\mathrm{kg\,m^{-3}}$), σ the surface tension ($\sigma = 7{\cdot}3 \times 10^{-2}\,\mathrm{N\,m^{-1}}$) and g the Earth's gravitational constant. For the velocity V we have used ($V = 800\,\mu\mathrm{m\,s^{-1}}$) this leads to a thickness $d \approx 1\,\mu\mathrm{m}$. After the evaporation of the water, we obtained a polymer film approximately 100 Å thick.

The glass slide covered with the polymer film was fixed to the pen-holder of a plotter and lay on a piece of velvet. When the pen-holder was moved, the polymer film is rubbed on the velvet. The trajectory of the pen-holder is determined by a function generator connected to the X and Y inputs of the plotter. The symmetry of this trajectory, which is the symmetry of the substrate obtained after rubbing, can thus be chosen among all the possible plane point groups by choosing the input functions.

2.2.2. *Rubbed polymer films having a C_{4v} symmetry*

When the rubbing trajectory is a succession of segments $\mathbf{r}_1$, $\mathbf{r}_2$, $-\mathbf{r}_1$ and $-\mathbf{r}_2$ with $|\mathbf{r}_1| = |\mathbf{r}_2|$ and $\mathbf{r}_1 \perp \mathbf{r}_2$, we obtain a film with a symmetry $C_{4v} = \{E, C_4, \hat{\sigma}_1, \hat{\sigma}_2, \hat{\sigma}'_1, \hat{\sigma}'_2\}$. C_4 is a fourfold symmetry whose axis $\mathbf{C}_4$ is perpendicular to the substrate surface. $\hat{\sigma}_1$, $\hat{\sigma}_2$, $\hat{\sigma}'_1$ and $\hat{\sigma}'_2$ are the symmetries in the planes σ_1, σ_2, σ'_1 and σ'_2; σ_1 and σ_2 contain the axis $\mathbf{C}_4$ and one of the rubbing directions, σ'_1 and σ'_2 contain the axis $\mathbf{C}_4$ and one of the bisectors of the rubbing directions (see figure 2 (*b*)). Note that the results do not depend on the order of the segments in the rubbing trajectory. This is true provided that the segmental lengths are not so large that the action of rubbing along one segment cancels the effect of rubbing along the former segments.

2.2.3. *Types of anchoring allowed by C_{4v} symmetry*

C_{4v} symmetry allows five types of anchoring according to the orientation of $\mathbf{n}_1$ with respect to the symmetry elements.

(*a*) In the general case there are eight possible anchoring directions tilted with respect to the plane S of the substrate surface.

(*b*) If $\mathbf{n}_1$ is parallel to S, the eight anchoring directions become identical two by two, because of the identity of $\mathbf{n}$ and $-\mathbf{n}$ in nematics. A planar quadristable anchoring is obtained.

(*c*) If $\mathbf{n}_1$ is tilted with respect to S and belongs to one of the mirror planes, there are four anchoring directions. Note that there are two possible anchorings of this type because there are two families of mirror planes in the symmetry elements: the anchoring directions may belong to the planes σ_1 and σ_2 or σ'_1 and σ'_2.

(*d*) If $\mathbf{n}_1$ is parallel to S and belongs to one of the mirror planes, there are two possible anchoring directions. As in the former case, there are two anchorings of this type.

(*c*) If $\mathbf{n}_1$ is parallel to $\mathbf{C}_4$ there is only one direction of anchoring; the anchoring is homeotropic.

We still have no way of determining *a priori* which of these types of anchoring is to be obtained on a given substrate having C_{4v} symmetry; the type of anchoring obtained has to be determined experimentally.

3. Wetting of substrates inducing a multistable anchoring

3.1. *Experimental method*

In order to determine the type of anchoring induced by a given substrate and to study the dependence of the chosen anchoring direction with the wetting conditions, we made nematic droplets spread on the substrate studied [4]. We have improved our method of droplet deposition in order to minimize the capillary oscillations of the free interface which create perturbations in the wetting textures [4].

Droplets of the nematic E8 (B.D.H. Chemicals) were formed at the end of a capillary tube. This tube was fixed to a stage having a vertical displacement which allows the capillary tube to be moved towards the substrate in a controlled manner. The motion of the capillary was stopped when the nematic droplet entered in contact with the substrate and the capillary was left at rest during the spreading of the nematic on the substrate; there were, therefore, no oscillations of the free interface driven by motions of the capillary during the spreading.

3.2. *Results*

3.2.1. *SiO films evaporated under oblique incidence*

200 Å thick SiO films induce an asymmetric tilted anchoring for incidence angles ε (see figure 2 (*a*)) between 60° and 72° [7]. The inside of nematic droplets spread on such films was separated into four domains, two having the orientation $\mathbf{n}_1$ and the other two the orientation $\mathbf{n}_2 = \hat{\sigma}\mathbf{n}_1$. The domains were separated by two walls: one diametral and the other having the shape of a cardioid (see figure 3). This texture is similar to the textures of spread droplets shown in [4] except for the following features:

(*a*) the walls separating the domains with different orientations do not make large scale zig-zags;
(*b*) no crescent-shaped domains are observed;
(*c*) no domains are created inside the cardioid.

This confirms the fact that these three features previously observed in the textures of spread droplets are due to oscillations of the nematic–air interface created by the motion of the capillary depositing the droplets.

The shape of the walls in the textures presented here are similar to that predicted by our model of anchoring selection (see figure 4) [4] except for two details:

(*a*) the experimentally observed walls show small scale zig-zags whose amplitudes increase at the periphery where the walls become erratic (see figure 3 (*a*));
(*b*) the predicted wall corresponding to the cardioid (see figure 4) does not have cusps when it intersects the diametral wall, as observed experimentally.

The first point can be explained by the presence of inhomogeneities in the SiO film creating a random contribution to the potential of interaction between the nematogenic molecules and the solid substrate [4]. We have no explanation for the second

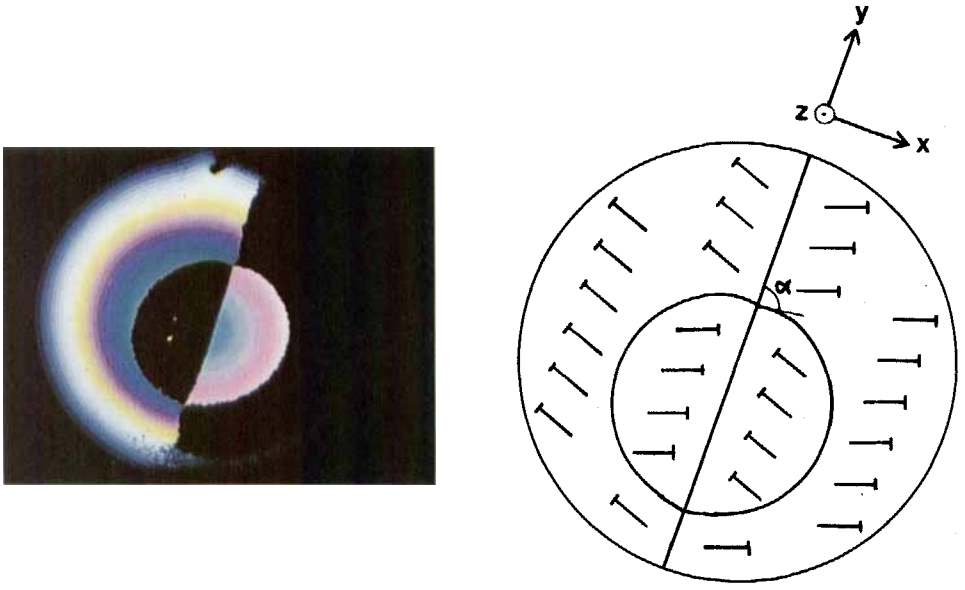

(*a*) (*b*)

Figure 3. Nematic droplet spread on an SiO film inducing an asymmetric tilted anchoring. (*a*) Droplet aspect observed with a polarizing microscope. (*b*) Nematic orientation inside the droplet.

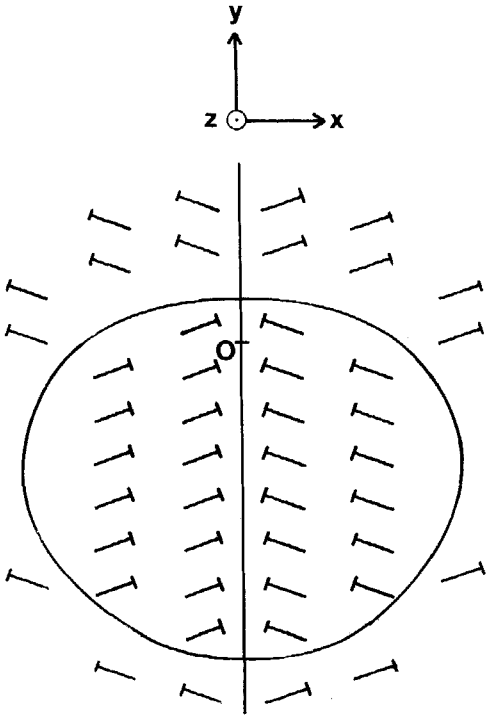

Figure 4. Prediction of the model for the shape of the walls appearing inside droplets spread on SiO films inducing an asymmetric tilted anchoring. O is the centre of the droplet.

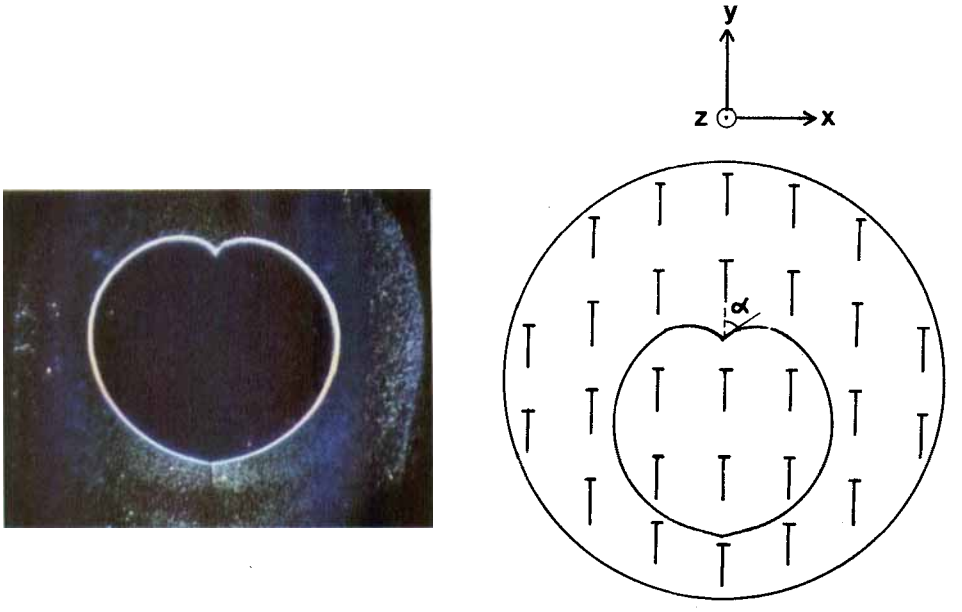

(*a*) (*b*)

Figure 5. Nematic droplet spread on an SiO film inducing a symmetric tilted anchoring. (*a*) Droplet aspect observed with a polarizing microscope. (*b*) Nematic orientation inside the droplet.

point. The appearance of the cusps changes with the angle of incidence of the evaporation ε; when ε is slightly greater than 60°, the anchoring directions are nearly perpendicular to the incidence plane σ [7]. The cusps are then hardly observable and the cardioid shaped wall is identical to that predicted by the model. When ε increases, the anchoring directions move towards the plane σ [7]; the angle of the cusp α decreases from 90°. When ε becomes equal to 72°, the anchoring becomes symmetric tilted [7]; α is then equal to 40° (see figure 5).

3.2.2. *Polymer films rubbed in two orthogonal directions*

When the droplets are observed between crossed polarizers with the rubbing directions along the bisectors of the polarizer directions, their inside is separated in four dark portions by a bright cross (see figure 6 (*a*)); the branches of the cross are parallel to the rubbing directions. This shows that there are four possible azimuthal orientations; $\varphi = 0, \pi/2, \pi$ and $3\pi/2$ (φ is measured from the Oy axis coinciding with one of the bisectors of the rubbing directions: (see figures 1 and 2 (*b*)). Using nematic cells limited by glass slides covered with polymer films and uniformly oriented [4], we have checked that the anchoring is planar. There are two possible anchoring directions parallel to the bisectors of the rubbing directions: this is the fourth type of anchoring described in §2.2.2.

This texture of the spread droplets is compatible with our model [4]. As predicted for planar anchorings, the anchoring direction depends only on the direction ψ of the wetting flow and not on its speed. According to the experimental results, the potential of interaction between the nematic and the polymer film has four minima located on the Ox and Oy axes. This potential has then four valleys separated by crest lines which are the great circles C_1 and C_2 contained in the planes σ_1 and σ_2

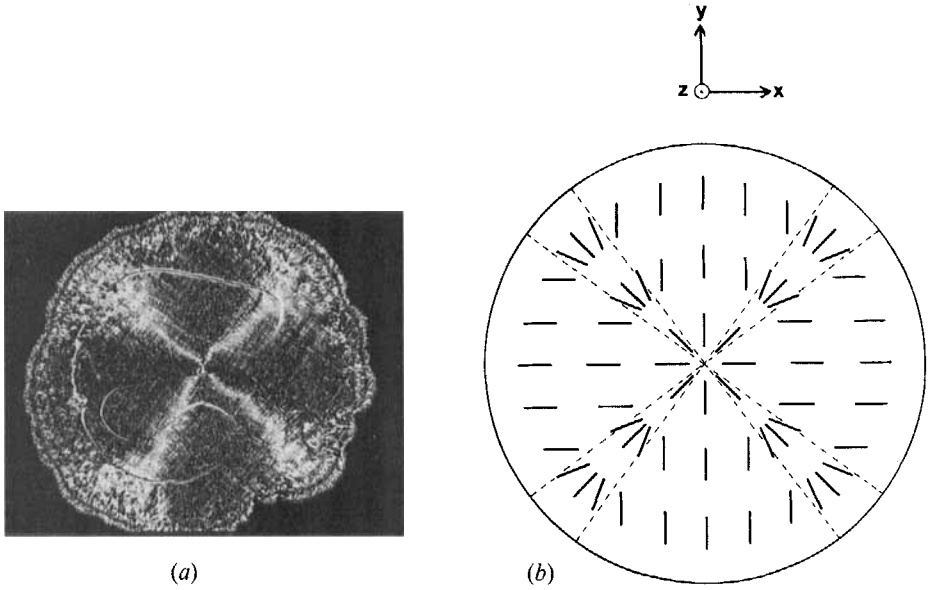

(a) (b)

Figure 6. Nematic droplet spread on a polymer film rubbed in two orthogonal directions. (*a*) Droplet aspect observed with a polarizing microscope. (*b*) Nematic orientation inside the droplet.

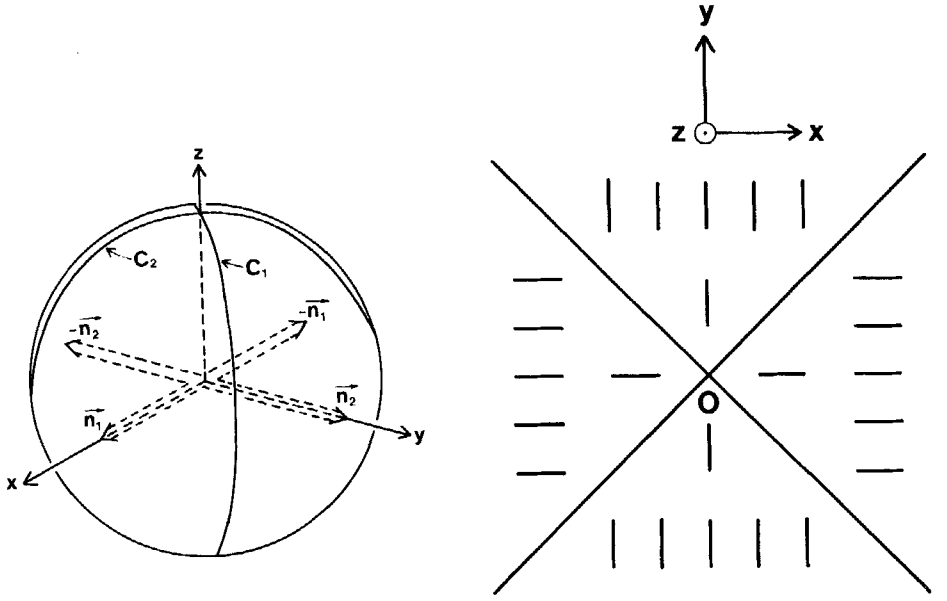

(a) (b)

Figure 7. Polymer film rubbed in two orthogonal directions. (*a*) Minima and crest-lines of the potential of interaction with the nematic. (*b*) Prediction of the nematic orientation inside the droplets.

(see figure 7(*a*)); Experimentally, the domains of different orientations are not separated by walls but by zones in which the orientation rotates of $\pi/2$ (see figure 6(*b*)).

4. Conclusion

We have studied the wetting by nematic droplets of SiO films evaporated under oblique incidence inducing a bistable anchoring and polymer films rubbed in two orthogonal directions. We have used a new method of droplet deposition which minimizes the capillary oscillations of the free nematic interface during the spreading of the droplets. For the first type of substrate, this method has allowed us to determine which of the accidents not predicted by our model of anchoring selection and previously observed in the walls separating domains of different orientations were due to oscillations of the free nematic interface during spreading. We find that only one accident (the cusps of the cardioid shaped wall) remains when using this method. As far as the second type of substrate is concerned, we have found that this substrate having C_{4v} symmetry induces a planar bistable anchoring. There are two possible anchoring directions which are parallel to the bisectors of the rubbing directions. The textures of the spread droplets are similar to that predicted by our model.

References

[1] De Gennes, P. G., 1985, *Rev. Mod. Phys.*, **57**, 827.
[2] Huk, C., and Scriven, L.,, 1971, *J. Colloid Interface Sci.*, **35**, 85.
[3] Dussan, V. F., and Davis, S., 1974, *J. Fluid Mech.*, **65**, 71.
[4] Jérôme, B., and Pieranski, P., 1988, *J. Phys., Paris*, **49**, 1601.
[5] Uchida, T., Ohgawara, M., and Wada, M., 1980, *Jan J. appl. Phys.*, **19**, 2127.
[6] Monkade, M., Boix, M., and Durand, G., 1988, *Europhysics Lett.*, **5**, 697.
[7] Jérôme, B., Pieranski, P., and Boix, M., 1988, *Europhysics Lett.*, **5**, 693.
[8] Yang, C. C., Josefowicz, J. Y., Alexandru, L., 1980, *Thin Solid Films*, **74**, 117.